EurJIC
European Journal of Inorganic Chemistry

Research Article
doi.org/10.1002/ejic.202400565

Chemistry Europe
European Chemical Societies Publishing

www.eurjic.org

High–Field EPR Studies on Three Binuclear μ–Oxo–Bridged Iron(III) Complexes: $Na_4[Fe(edta)]_2O\cdot 3H_2O$, $[Fe(phen)_2(H_2O)]_2O(NO_3)_4\cdot 5H_2O$ and $[Fe(salen)]_2O$

Andrew Ozarowski*[a]

A High–Field, High–Frequency Electron Paramagnetic Resonance (HFEPR) study was performed on the binuclear μ–oxo bridged complexes $Na_4[Fe(edta)]_2O\cdot 3H_2O$, $[Fe(phen)_2(H_2O)]_2O(NO_3)_4\cdot 5H_2O$ and $[Fe(salen)]_2O$, where edtaH_4 = ethylenediaminetetraacetic acid, phen = 1,10–phenanthroline and salenH_2 is NN′–ethylenebis(salicylideneimine). The spin Hamiltonian parameters were determined for the thermally excited spin states with spin S = 1, 2 and 3. The contributions to the zero–field splitting due to the local zero field splitting on individual iron ions and to the anisotropic metal–metal interactions were evaluated. Surprisingly large magnitudes of the anisotropic exchange interactions were found.

Introduction

A large number of the binuclear iron(III) complexes with a single μ–oxo bridge have been known for decades.[1–8] They have been studied because of their relevance to biological systems, their importance for the theory of the intramolecular exchange interactions and their possible catalytic activity. A wide variety of ligands are able to form such binuclear compounds, including 2,2′–bipyridine, 1,10–phenathroline, 2,2′,2″–terpyridine, Schiff bases, porphyrins and artificial aminoacids like the well–known edta. A multitude of typical techniques, IR, UV–VIS spectroscopy, and magnetic measurements was employed. In addition, the isotropic paramagnetic shift of the proton magnetic resonance signals was investigated in some μ–oxo Fe(III) dimers including $[Fe(salen)]_2O$[9] studied here. Notably, EPR spectroscopy was very rarely used, an exception being the pioneering study by Okamura and Hoffman.[10] The complexes studied in this work are $Na_4[Fe(edta)]_2O\cdot 3H_2O$,[11,12] $[Fe(phen)_2(H_2O)]_2O(NO_3)_4\cdot 5H_2O$[11,13] and $[Fe(salen)]_2O$,[14] where edtaH_4 = ethylenediaminetetraacetic acid, phen = 1,10–phenanthroline and salenH_2 is NN′–ethylenebis(salicylideneimine), which is a Schiff base–a condensation product of salicylaldehyde and ethylenediamine. The three complexes exhibit typical properties of their family–they are intramolecular antiferromagnets with strong metal–metal interactions. The Fe–O_{bridge} distance is 1.78 ± 0.01 Å and the FeOFe bridge is bent in each case. A strong infrared ν_{as}(FeOFe) band at 851 cm^{-1}, 827 cm^{-1} and 832 cm^{-1} was observed in the edta,[12] phen[13] and salen[14b] complexes, respectively. More details can be found in comprehensive reviews.[1–5]

[a] A. Ozarowski
National High Magnetic Field Laboratory, Florida State University, 1800 East Paul Dirac Drive, Tallahassee, FL 32310 USA
E-mail: ozarowsk@magnet.fsu.edu

Supporting information for this article is available on the WWW under https://doi.org/10.1002/ejic.202400565

Magnetic Properties of the Binuclear μ–oxo Bridged Iron(III) Complexes

The FeOFe bridge in the single–bridged μ–oxo systems is almost always bent with the FeOFe angle over a range ~130 to 180 deg.[1,2] The bridge provides a pathway for relatively strong antiferromagnetic exchange interactions which are described by the Heisenberg–Dirac–van Vleck Hamiltonian[15]

$$\hat{H} = J\hat{S}_1\hat{S}_2 \tag{1}$$

Since other conventions are encountered in the literature, like $-J\hat{S}_1\hat{S}_2$ and $-2J\hat{S}_1\hat{S}_2$, readers should always check the notation used in a particular paper. Using $+J\hat{S}_1\hat{S}_2$ is natural when analyzing the anisotropic metal–metal interactions in addition to the isotropic term,[15] see Equations (5) and (6) below. It is convenient to define the total spin operator of the binuclear system:

$$\hat{S} = \hat{S}_1 + \hat{S}_2 \tag{2}$$

The total spin quantum number S may assume values 0, 1, 2, 3, 4 and 5. The S = 0 state is the ground state if $J > 0$. The energies of the spin states can be found from

$$E_S = \frac{J}{2}\{S(S+1) - S_1(S_1+1) - S_2(S_2+1)\} \tag{3}$$

where $S_1 = S_2 = 5/2$ for Fe^{3+}. In this way, the excited states with S = 1, 2, 3, 4, and 5 lie J, 3 J, 6 J, 10 J and 15 J, respectively, above the ground S = 0 state. The exchange integral J in such μ–oxo bridged iron(III) complexes tends to assume values around 200 cm^{-1}. Magnetic susceptibility approaches zero at very low temperatures and rises with increasing temperature to reach at 300 K about 0.0016 cgs emu, corresponding to an effective magnetic moment of 1.95 μ_B per one Fe^{3+} ion, compared to 5.9 μ_B for monomeric Fe^{3+} complexes.

Research Article
doi.org/10.1002/ejic.202400565

The Zero–Field Splitting (ZFS)

Electron Paramagnetic resonance (EPR) is an extremely valuable tool for studies on chemical systems containing unpaired electrons. Over the decades, it has been used to study the electron density distribution, magnetic properties, exchange interactions, etc. in many systems, including free radicals and transition metal compounds with the d^1–d^9 electron configurations. Most of EPR is done at X–band (9.5 GHz, 0.3 cm^{-1}) or Q–Band (34 GHz, 1.1 cm^{-1}), but these resonant energies have limitations for studying states with a spin number $S > 1/2$ in any systems (monomeric or polymeric). The states with a spin number $S > 1/2$ may split at zero magnetic field into $2S+1$ M_S levels, with M_S ranging from $-S$ to S, which is referred to as the zero–field splitting (ZFS).[15] The zero–field splitting is caused by the combined effect of the spin–orbit coupling and ligand field splitting. The ZFS energies are sometimes small, and in many cases EPR can be observed using the standard equipment, like the X Band or Q Band. In the Kramers–type ions (where S is an odd multiple of $\frac{1}{2}$), there are unsplit pairs of levels with M_S and $-M_S$ at zero magnetic field, like $\pm 1/2$ and $\pm 3/2$ in Co(II) (d^7, $S = 3/2$), referred to as Kramers doublets.[15] This guarantees observation of the EPR transitions within these doublets at any microwave frequency, no matter how low. However, for non–Kramers ions (S integer), such unsplit doublets are not present, and even in systems as simple as the mononuclear nickel(II) complexes with $S = 1$, the splitting between the M_S levels at zero magnetic field may be of the order of several wavenumbers, rendering the classical X and Q Band instrumentation useless.

The binuclear μ–oxo bridged iron(III) complexes studied in this work belong to the class of non–Kramers systems. Determination of the ZFS magnitude in such compounds has been attempted in the literature,[10,11,16] with limited success as the splitting in the first thermally accessible state with $S = 1$ proved to be large, beyond the reach of the standard X– or Q–Band EPR.

The EPR spectra of systems with the zero–field splitting are interpreted in terms of the spin Hamiltonian[15]

$$\widehat{\boldsymbol{H}} = \mu_B B\{\boldsymbol{g}\}\widehat{\boldsymbol{S}} + D_S\left\{\widehat{\boldsymbol{S}}_z^2 - \frac{1}{3}S(S+1)\right\} + E_S\left(\widehat{\boldsymbol{S}}_x^2 - \widehat{\boldsymbol{S}}_y^2\right) + B_4^0\boldsymbol{O}_4^0 + B_4^0\boldsymbol{O}_4^0 \quad (4)$$

$\widehat{\boldsymbol{S}}$ and its components in Equation (4) represent the total spin (see Equation (2)). D, E and B_4^0, B_4^4 are the zero–field splitting parameters. $\boldsymbol{O}_4^0$and $\boldsymbol{O}_4^4$ are the Stevens operators.[15,17] The quartic parameters B_4^0, B_4^4 are only applicable for $S > 3/2$ but they are not always needed even in such cases. In binuclear complexes, each spin state S has its own set of parameters (accordingly, D_S and E_S appear in Equation (4) rather than simply D and E). The spin Hamiltonian (4) when applied to polynuclear complexes is often referred to as the "giant spin" Hamiltonian.

The High–Field, High–Frequency EPR (HFEPR) operates at frequencies of hundreds of Gigahertz or more and uses very high magnetic fields. The instrument used in this research can reach a magnetic field of 15 Tesla. Very large microwave quantum energy (like 20 cm^{-1} at 600 GHz) makes the EPR studies possible in complexes of Ni(II), Fe(II), Mn(III), Cr(II), V(III) and Ti(II) and transitions in complexes under study here should also be observable.[18]

The author has performed in the past single–crystal X–Band EPR studies on two μ–oxo complexes, $Na_4[Fe(edta)]_2O\cdot 3H_2O$ (Figure 1) and $[Fe(phen)_2]_2O(NO_3)_4\cdot 7H_2O$ (Figure 2).[11] The X–Ray structures of the edta and phen complexes were described in refs [11] and [13], respectively. The single–crystal X–Band EPR study allowed determination of the D and E parameters in the spin states $S = 2$ and $S = 3$ of each complex.[11] The $S = 1$ state was not seen because of its too large ZFS parameters. In the case of the phen complex, one very intense resonance was observed at the end of the available magnetic field (1.5 T), and it was assigned to the $S = 1$ state. The amount of information was insufficient, however, to find the spin Hamiltonian parameters of the $S = 1$ state. It will be shown below that HFEPR was able to accomplish that task. In an X and Q–Band EPR study[16] on $[enH_2][Fe(hedta)\}_2O]\cdot 6H_2O$, where $hedtaH_3$ = hydroxyethylethylenediaminetriacetic acid, the D and E parameters for the $S = 1$, 2 and 3 states were determined, although the authors stated that the $S = 1$ parameters were "somewhat tenuous due to the paucity and broadness of these resonances".[16] If these parameters for $S = 1$ are correct, then they are exceptionally small in

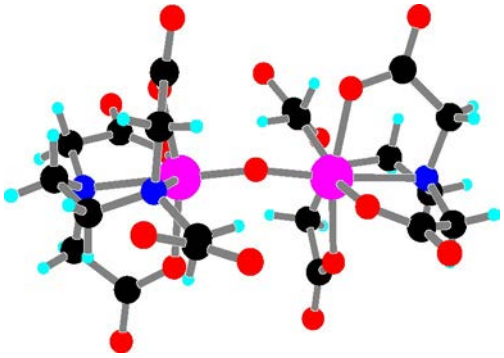

Figure 1. Structure of the $[Fe(edta)]_2O^{4-}$ anion in $Na_4[Fe(edta)]_2O\cdot 3H_2O$.[11] The picture was generated from the CSD_CIF_ZIDVUD data in the Cambridge Crystallographic Data Centre. The FeOFe angle is 163.2 deg.

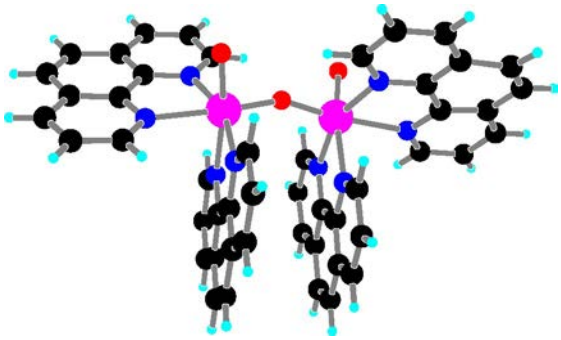

Figure 2. Structure of the $[Fe(phen)_2(H_2O)]_2O^{4+}$ cation in $[Fe(phen)_2(H_2O)]_2O(NO_3)_4\cdot 5H_2O$.[13] The picture was generated from the CSD_CIF_CUJFAO data of the Cambridge Crystallographic Data Centre. The FeOFe angle is 155 deg. Note that the aquo–hydrogen atoms coordinates have not been determined.

Research Article
doi.org/10.1002/ejic.202400565

this family of compounds (Table 1 below), and this made the observation of S = 1 in Q–Band EPR possible. The hedta complex was also studied earlier by single–crystal Q–Band EPR leading to the determination of $D = 0.15\ cm^{-1}$ in S = 2.[10] Also, a 1976 paper[19] describes determination of D and E in the S = 2 state of a compound formulated as $Na_4[Fe(edta)]_2O \cdot 12H_2O$, which may be the same species as the edta complex in this paper, despite the difference in the reported number of water molecules in the formula. The reported D of $0.21\ cm^{-1}$ is close to the value in Table 1, while E of $0.015\ cm^{-1}$ is substantially different. References [10, 11, 16 and 19] appear to be the only ones in which interpretation of the EPR spectra of the single–bridged μ–oxo iron(III) complexes was attempted. Occasionally, the ZFS in Fe^{3+} dimers was also studied by the single–crystal magnetic susceptibility measurements like it was done for the $[Fe(salen)]_2O$ complex[14] (Figure 3). Taking into account the scarcity of the EPR studies and the persistent interest in this class of binuclear complexes,[4–8,20] this author has performed a HFEPR study on the binuclear iron(III) complexes of edta, phen and salen discussed above to determine the spin Hamiltonian parameters which have been inaccessible in the past and to make more researchers aware of this relatively new instrumental method.

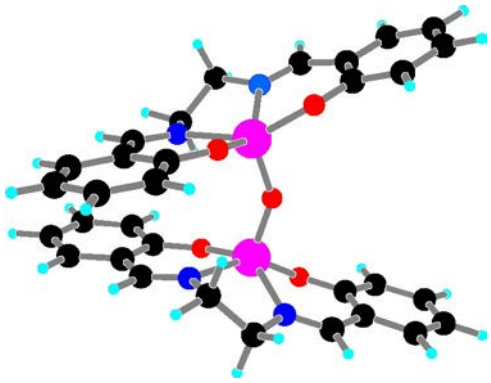

Figure 3. Structure of the $[Fe(salen)]_2O$.[21] The picture was generated from the OFESAL (CCDC 1225740) data of the Cambridge Crystallographic Data Centre. The FeOFe angle is 144.6 deg.

Experimental

The powder samples of the $Na_4[Fe(edta)]_2O \cdot 3H_2O$ and $[Fe(phen)_2(H_2O)]_2O(NO_3)_4 \cdot 5H_2O$ complexes which were synthesized for the 1995 paper[11] were used in this work. They did not show any signs of degradation, as proven by their X–Band EPR and HFEPR spectra The $[Fe(salen)]_2O$ compound was synthesized as described in the literature and was easily obtained in very pure crystalline form both as a dichloromethane solvate[14] and as a solvent–free species.[21] These two species exhibited HFEPR spectra of the same nature but differing in their spin Hamiltonian parameters.

Table 1. Spin Hamiltonian parameters. Estimated errors in the last shown digit are given in parentheses.

Sample, temperature and spin state	g_x	g_y	g_z	D, cm^{-1}	E, cm^{-1}	B_4^0, B_4^{4}[a] $10^{-4}\ cm^{-1}$
$Na_4[Fe(edta)]_2O(H_2O)_3$						
285 K, S = 1	2.012(1)	2.012(1)	2.003(1)	5.331(2)	0.706(2)	–
285 K, S = 2	2.006(2)	2.004(1)	2.010(1)	0.241(1)	0.063(1)	0.6(3), 10(3)
S = 2 ref [11]	2	2	2	0.2477	0.0598	1.3, 31.4
285 K, S = 3	2.008(1)	2.008(1)	2.004(1)	0.608(1)	0.018(1)	−0.8(1), 0 [b]
S = 3 ref [11]	2	2	2	0.6044	−0.0158	−0.9, 0.3
100 K S = 1	2.013(1)	2.012(2)	2.003(2)	5.309(6)	0.671(3)	–
$[Fe(phen)_2(H_2O)]_2O(NO_3)_4(H_2O)_5$						
300 K, S = 1	2.013(1)	2.013(1)	2.003(1)	4.776(1)	0.359(1)	–
300 K, S = 2	2.012(1)	2.012(1)	2.003(1)	0.259(1)	0.036(1)	3.0(2), 0(1)
S = 2 ref [11]	2	2	2	0.2562	0.0372	4.0, −1.8
300 K, S = 3	2.012(1)	2.010(1)	2.004(1)	0.686(1)	0.0084(3)	−0.30(5), 0[b]
S = 3 ref [11]	2	2	2	0.686	0.0079	−0.3, 0.9
150 K S = 1	2.013(1)	2.013(1)	2.003(1)	4.645(1)	0.374(2)	–
$[Fe(salen)]_2O$						
308 K, S = 1	2.010(1)	2.012(1)	2.000(2)	10.106(2)	1.694(2)	–
308 K, S = 2	2.003(2)	2.005(1)	2.006(1)	0.689(1)	0.223(1)	−14(1), −0.8(4)
308 K, S = 3	_[c]	_[c]	2.002(1)	0.458(2)	_[c]	0.3(1), 0 [b],[c]
150 K, S = 1	2.011(2)	2.009(2)	2.021(4)	10.255(1)	1.816(1)	–
150 K, S = 2	2.006(1)	2.006(1)	2.002(1)	0.738(6)	0.218(2)	−9(1),−19(1)
$[Fe(salen)]_2O \cdot CH_2Cl_2$						
300 K S = 1	2.013(8)	2.005(9)	2.02(2)	10.66(3)	0.57(2)	–
150 K S = 1	2.008(2)	2.011(2)	2.001(7)	10.924(4)	0.644(4)	–
$[enH_2][Fe(hedta)_2O] \cdot 6H_2O$						
S = 1 ref [16]	2	2	2	1.950	0.650	
S = 2 ref [10, 16]	2	2	2	0.150	0.0195	
S = 3 ref [16]	2	2	2	0.57	0	

[a] Only applicable to S = 2 and S = 3. [b] B_4^4 assumed 0, not fitted. [c] Only g_z, D and B_4^0 could be determined.

Research Article
doi.org/10.1002/ejic.202400565

The HFEPR spectra were recorded on the home–built transmission instrument at the NHMFL.[22] The microwaves were generated by the Virginia Diodes sources which employed an 8–20 GHz base frequency generator connected to a chain of frequency multipliers (doublers and triplers) creating frequencies over the range 26 to 650 GHz (however, with gaps). The instrument uses no resonance cavity. A superconducting Oxford Instruments magnet could reach magnetic field of 15 Tesla. The instrument is equipped with a cryostat working between 3 and 310 K.

The simulations of the HFEPR spectra were accomplished using the author's own software.[23]

Results and Discussion

The exchange integral *J* values have been determined in the literature for all compounds reported here. The complexes of edta,[12] phen[24] and salen[14] exhibited *J* of 198 cm^{-1}, 220 cm^{-1} and 174 cm^{-1}, respectively. These numbers are compatible with the HDVV Hamiltonian (1) used in this paper and were converted from the literature data when needed. With these *J* values, the excited spin states with S equal to 1, 2 and 3 are thermally accessible at the room temperature and are expected to produce HFEPR spectra. Temperature lowering causes these states to be depopulated but weak EPR signals due to S = 1 could be observed even at 50 K (Figures 8 and S2). The HFEPR spectra showed surprisingly good resolution allowing identification of the features associated with the triplet (S = 1), quintet (S = 2) and septet (S = 3) states and leading to successful determination of the spin Hamiltonian parameters in each spin state in the edta and phen complexes. The spectra of the salen complex were somewhat less resolved so that the parameters of the S = 3 state could be only partially determined, only in the solvent–free species. Still, the spectra of S = 1 and S = 2 states were convincingly simulated. The solvated species was even more problematic so that only the state S = 1 could be analyzed at 300 K and 150 K. The spectra are shown in Figures 4, 5, 7, 8 and in the ESI. The spin Hamiltonian parameters were determined by fitting a dataset consisting of resonance fields observed at many frequencies, as shown in Figure 6 for the phen complex. Plots for the other two compounds can be seen in the ESI.

A comment may be useful here for readers less familiar with the topics. Randomly oriented microcrystallites contribute to an EPR spectrum of a powder sample. The EPR resonance fields are extremely sensitive to the orientation of a molecule versus the magnetic field. The features observed in a powder EPR spectrum correspond to the molecular orientations at which the EPR resonance positions are weakly dependent on orientation. This happens at the "turning points" when the resonances pass through maximum or minimum magnetic field at the X, Y and Z orientations, but sometimes such "turning points" occur also between the molecular axes, a good example being the "half–field" $\Delta M_S = 2$ transition observed in this paper (see Figures S13, S14).

A powder EPR simulation involves calculating thousands of the "single–crystal" spectra at different orientations defined by the polar angles θ and Φ, multiplying each of them by a factor

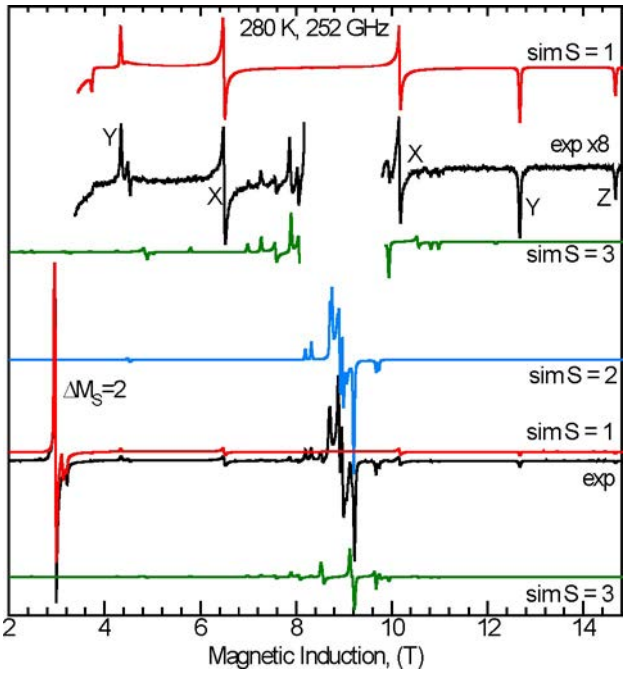

Figure 4. HFEPR spectra of $Na_4[Fe(edta)]_2O \cdot 3H_2O$. Black: experimental; red, blue and green: simulated for the S = 1, S = 2 and S = 3 state, respectively. The upper part shows a magnified experimental spectrum with the strongest signals cut off and the simulated traces for S = 1 and S = 3 scaled to match the magnified spectrum amplitude. Labels X, Y and Z indicate the molecular orientations at which the S = 1 transitions occur. $\Delta M_S = 2$ is a "forbidden" transition also known as a "half–field transition", which is typically very strong in the spectra of the S = 1 states. See also Figure S5.

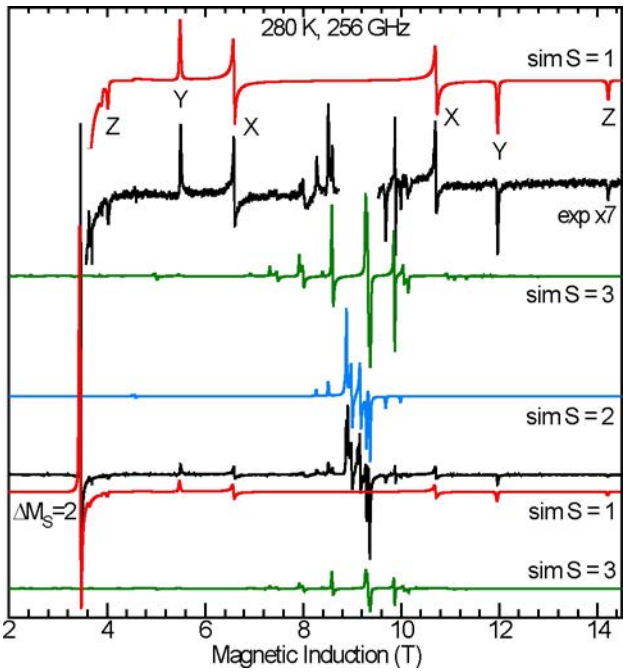

Figure 5. HFEPR spectra of $[Fe(phen)_2(H_2O)]_2O(NO_3)_4 \cdot 5H_2O$. Black: experimental; red, blue and green: simulated for the S = 1, S = 2 and S = 3 state, respectively. The upper part shows a magnified experimental spectrum with the strongest signals cut off and the simulated traces for S = 1 and 3 states scaled to match the magnified spectrum amplitude. Labels X, Y and Z indicate the molecular orientations at which the S = 1 transitions occur. See also Figure S7.

Research Article
doi.org/10.1002/ejic.202400565

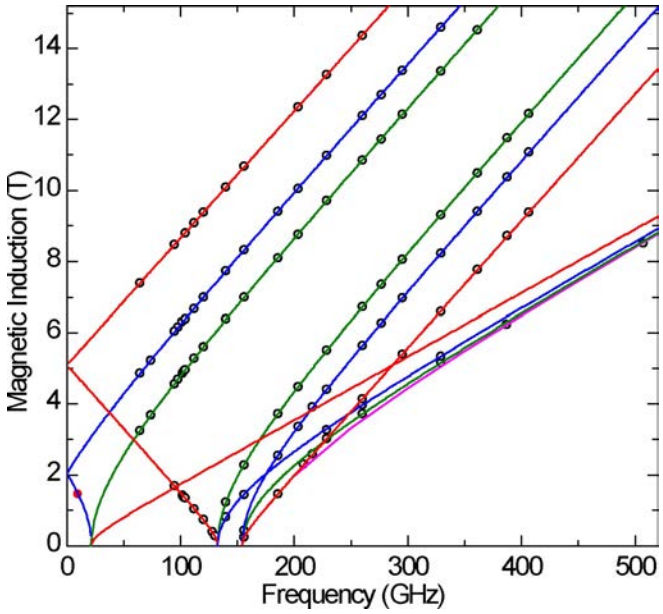

Figure 6. Resonance field versus microwave frequency dependencies observed for the S = 1 state in $[Fe(phen)_2(H_2O)]_2O(NO_3)_4 \cdot 5H_2O$ at room temperature. The green, blue and red lines are calculated for the molecular orientations X, Y and Z, respectively, using parameters in Table 1. The purple line shows the off–axial $\Delta M_S = 2$ transition at positions read out from the simulated powder spectra. The open black circles represent the experimental HFEPR resonances. The red filled circle at 9.781 GHz, 1.468 T shows the only S = 1 transition observed in X–Band EPR,[11] which can now be identified as a Y feature. The three frequencies at which resonances occur at zero magnetic field correspond to energies 2 *E* (0.718 cm^{-1}, 21.54 GHz), *D*–*E* (4.417 cm^{-1}, 132.51 GHz) and D + E (5.134 cm^{-1}, 154.02 GHz).

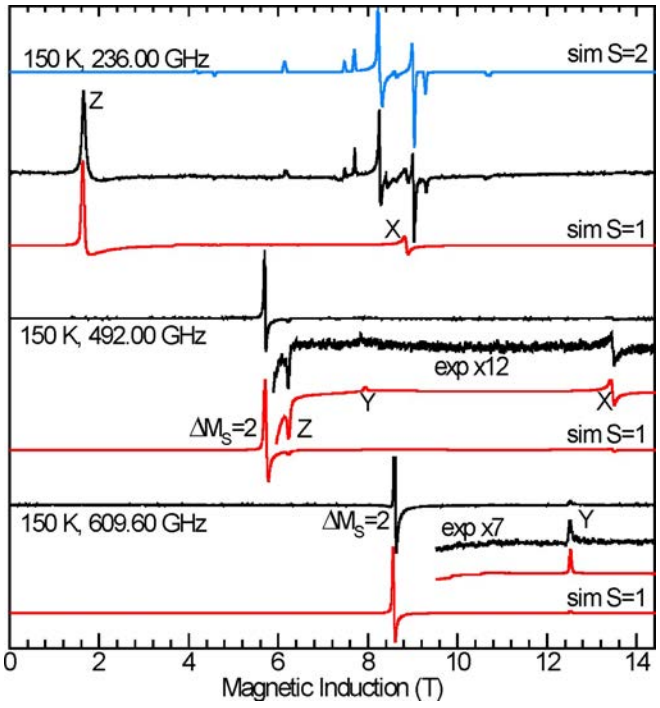

Figure 7. HFEPR spectra of $[Fe(salen)]_2O$ recorded at 150 K with various microwave frequencies. Black: experimental; red: simulated S = 1 state; blue: simulated S = 2 state. Magnified experimental and simulated traces are shown for the 492.00 and 609.60 GHz spectra. Labels X, Y and Z indicate the molecular orientations at which the S = 1 transitions occur.

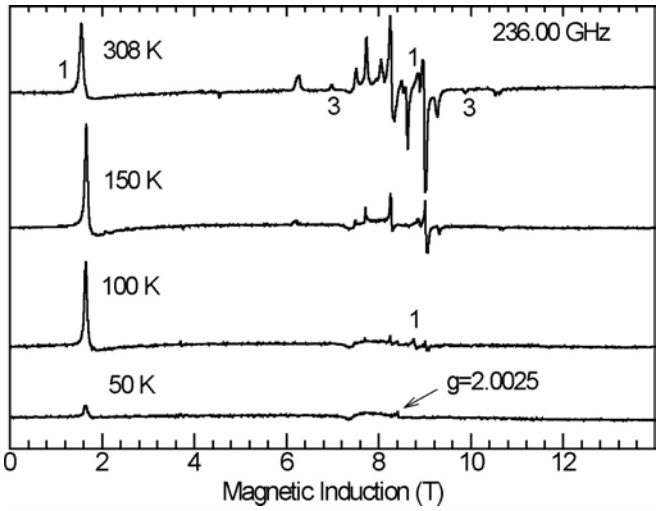

Figure 8. HFEPR spectra of solvent-free $[Fe(salen)]_2O$ recorded at various temperatures. Labels 1 and 3 indicate the spin state in which these transitions occur. The remaining features in the central part of the spectrum are due to S = 2. The change in the lowest–field transition position is caused by a slight temperature dependence of the spin Hamiltonian parameters (Table 1). At 50 K, a trace of a radical appears at g = 2.0025, whereas the S = 2 and S = 3 features are not visible any longer.

$\sin\theta d\theta d\Phi$ and adding them together. When calculating a spectrum at an orientation, the resonance fields are found first, then the eigenvectors of the levels involved in an EPR transition are determined at the appropriate resonance field and the transition probability is calculated (Figures S11, S12). The populations of the states involved in a transition are also taken into account to finally determine the resonance intensities. The resonance fields at an orientation are found in an iterative procedure which involves multiple diagonalizations of the spin Hamiltonian matrix (which in general contains complex numbers). Figure 4 presents the experimental spectrum of $Na_4[Fe(edta)]_2O \cdot 3H_2O$ and separately simulated spectra of the S = 1, S = 2 and S = 3 states. Figure S5 in the ESI shows a simulated spectrum obtained by summing these three simulated spectra multiplied by the populations of the respective spin states.

The Spin Hamiltonian Parameters

Table 1 presents the spin Hamiltonian (4) parameters found in this work and in references [10, 11 and 16]. It is important to understand that the signs of the zero–field splitting parameters *D*, *E*, B_4^0 and B_4^4 are relative. Changing the sign of all of them at the same time will not result in a different simulation. As seen in Table 1, the *g* values in each spin state of each complex are very close to the free–electron value $g_e = 2.0023$, but the deviations of the *g* components from that value cannot be ignored in simulations of the HFEPR spectra, opposite to what was done in the past for the X and Q band spectra.[10,11,16,19] With frequency of ~200 GHz the HFEPR is ~20 times more sensitive to *g* than is the X–Band EPR (~9.5 GHz). The zero–field splitting parameter $D_{S=1}$ in the triplet (S = 1) states is very large, around 5 cm^{-1} for the edta and phen complexes and more than

10 cm^{-1} in the salen complex, explaining why the triplet spectra were not observed in the past. The quintet state $D_{S=2}$ values are the smallest ones in each case, whereas $D_{S=3}$ and $E_{S=3}$ values in the septet state are of intermediate magnitudes. The *D* and *E* values are slightly temperature dependent, but there is no uniform trend. $D_{S=1}$ the edta species drops by 0.4% between 295 and 100 K, in phen it drops by 3% between 300 and 150 K, and finally in the salen complex it increases by 1.4% when temperature changes from 308 to 150 K.

The room–temperature parameters in Table 1 for the spin states 2 and 3 in the edta and (particularly) phen complex are very similar to those found in ref [11]. Figure S1 in the ESI shows the X–Band spectra of the edta and phen complexes simulated by using parameters from Table 1.

The "giant spin" Hamiltonian (4) allows determination of the zero–field splitting parameters in different spin states of a dimeric complex, which are shown in Table 1. However, one needs to resort to the "microscopic" spin Hamiltonian (5) to understand the nature of these parameters. The S = 5/2 state of the Fe^{3+} ions undergoes zero field splitting which may be thus called local zero–field splitting. This local zfs contributes to the zero–field splitting of the dimer spin states (see Formulas 6 below). Another contribution is associated with the anisotropic metal–metal interactions which include the magnetic dipole–dipole interaction and the anisotropy of the exchange interactions. Instead of using the "giant spin" Hamiltonian (Equation (4)), one could apply (at least in theory) a spin Hamiltonian which is expressed in the spin operators $\hat{\boldsymbol{S}}_1$ and $\hat{\boldsymbol{S}}_2$ of two ions and operates within a set of 36 $|M_{S1}, M_{S2}>$ function of the binuclear Fe^{3+} system.

$$\widehat{H} = \mu_B \boldsymbol{B}\{\boldsymbol{g}_1\}\widehat{\boldsymbol{S}}_1 + D_{Fe1}\left\{\widehat{S}_{z1}^2 - \frac{1}{3}S(S+1)\right\} + E_{Fe1}\left(\widehat{S}_{x1}^2 - \widehat{S}_{y1}^2\right) +$$
$$\mu_B \boldsymbol{B}\{\boldsymbol{g}_2\}\widehat{\boldsymbol{S}}_2 + D_{Fe2}\left\{\widehat{S}_{z2}^2 - \frac{1}{3}S(S+1)\right\} + E_{Fe2}\left(\widehat{S}_{x2}^2 - \widehat{S}_{y2}^2\right) +$$
$$D_{12}\left\{\widehat{S}_{z1}\widehat{S}_{z2} - \frac{1}{3}\widehat{\boldsymbol{S}}_1\widehat{\boldsymbol{S}}_2\right\} + E_{12}\left(\widehat{S}_{x1}\widehat{S}_{x2} - \widehat{S}_{y1}\widehat{S}_{y2}\right) + J\widehat{\boldsymbol{S}}_1\widehat{\boldsymbol{S}}_2 \quad (5)$$

The microscopic spin Hamiltonian contains terms like those in Equation (4), for each of the Fe^{3+} ions plus the interaction terms (third line). The systems studied here lack any symmetry elements higher than C_1 and thus there is no guarantee that the local D_{Fe1} equals D_{Fe2} or that the local E_{Fe1} equals E_{Fe2}. The parameters *J*, D_{12} and E_{12} refer to the interactions between the two iron ions. The microscopic spin Hamiltonian can also be written in a tensor form to account for the fact that the *D* and *E* parameters for each of the Fe^{3+} ions and for the interaction terms may refer to different systems of coordinates.

$$\widehat{H} = \mu_B \boldsymbol{B}\{\boldsymbol{g}_1\}\widehat{\boldsymbol{S}}_1 + \widehat{\boldsymbol{S}}_1\{\boldsymbol{D}_{Fe1}\}\widehat{\boldsymbol{S}}_1 + \mu_B \boldsymbol{B}\{\boldsymbol{g}_2\}\widehat{\boldsymbol{S}}_2 + \widehat{\boldsymbol{S}}_2\{\boldsymbol{D}_{Fe2}\}\widehat{\boldsymbol{S}}_2 + \widehat{\boldsymbol{S}}_1\{\boldsymbol{D}_{12}\}\widehat{\boldsymbol{S}}_2 + J\widehat{\boldsymbol{S}}_1\widehat{\boldsymbol{S}}_2 \quad (5a)$$

It must be underscored here that the "microscopic" Hamiltonian is a correct approach, which unfortunately is prohibitively difficult. The "giant spin" Hamiltonian was introduced to make the problem of a dimer EPR spectrum manageable – instead of dealing with the 36x36 matrix of the microscopic Hamiltonian one just needs 3x3, 5x5 and 7x7 matrices for the dimer spin states S = 1, 2 and 3, respectively. When the isotropic exchange energy described by *J* is sufficiently larger than the zero–field splitting and Zeeman energy, the parameters of the microscopic (Equation (5) and (5a)) and the giant spin (Equation (4)) Hamiltonian are related by formulas (6). The coefficients below are correct only for an interaction between two S = 5/2 ions.[15] Reference [15] gives a comprehensive list of the coefficients for other dimeric systems, including non–symmetric dimers, for example d^3–d^5.

$$D_{S=1} = -3.2D_{Fe1} - 3.2D_{Fe2} + 3.7D_{12}$$
$$D_{S=2} = -(10/21)D_{Fe1} - (10/21)D_{Fe2} + (41/42)D_{12}$$
$$D_{S=3} = -(1/45)D_{Fe1} - (1/45)D_{Fe2} + (47/90)D_{12} \quad (6)$$

It should be emphasized that the coefficients in equations above apply also to the *E* values as well as to the elements of the zero–field splitting tensors $\{\boldsymbol{D}_{Fe1}\}$, $\{\boldsymbol{D}_{Fe2}\}$ and $\{\boldsymbol{D}_{12}\}$. The relations between the $\{\boldsymbol{D}\}$ tensor elements and the scalar parameters *D* and *E* are given below in formulas (7).

In the discussion below we will use a combined local tensor $\{\boldsymbol{D}_{Fe}\} = (\{\boldsymbol{D}_{Fe1}\} + \{\boldsymbol{D}_{Fe2}\})/2.$ = Relations (6) will thus change to

$$\{\boldsymbol{D}_{S=1}\} = -6.4\{\boldsymbol{D}_{Fe}\} + 3.7\{\boldsymbol{D}_{12}\}$$
$$\{\boldsymbol{D}_{S=2}\} = -(20/21)\{\boldsymbol{D}_{Fe}\} + (41/42)\{\boldsymbol{D}_{12}\}$$
$$\{\boldsymbol{D}_{S=3}\} = -(2/45)\{\boldsymbol{D}_{Fe}\} + (47/90)\{\boldsymbol{D}_{12}\} \quad (6a)$$

As the $\{\boldsymbol{D}_{Fe1}\}$, $\{\boldsymbol{D}_{Fe2}\}$ and $\{\boldsymbol{D}_{12}\}$ tensors and the resulting $\{\boldsymbol{D}_{S=1}\}$, $\{\boldsymbol{D}_{S=2}\}$ and $\{\boldsymbol{D}_{S=3}\}$ tensors are likely to operate in different coordinate systems, the task of determining them is practically insolvable, particularly in the absence of single–crystal EPR data. We will try, nevertheless, to make some estimations in the case of the phen complex. It was found experimentally that the $\{\boldsymbol{D}_{S=2}\}$ and $\{\boldsymbol{D}_{S=3}\}$ interactions operate in the same coordinates.[11] Moreover, although no parameters for the triplet state could be determined in ref [11], one transition in the S = 1 state was observed close to the upper limit of the available magnetic field for a limited range of the single crystal orientations. That transition passed through its lowest–field position at the same crystal orientation at which the S = 2 and S = 3 signals passed through their extremal positions (Figure 3 in ref [11]). This means that the ZFS interaction in the triplet state also operates in the same coordinates. This X-Band resonance was now shown to be a "Y" feature, see Figure 6. Thus, we will convert the *D* and *E* parameter sets for S = 1 and S = 2 to the corresponding diagonal tensor components. This can be accomplished using formulas (7)

Research Article
doi.org/10.1002/ejic.202400565

$$D_{xx} = -\frac{D}{3} + E$$

$$D_{yy} = -\frac{D}{3} - E$$

$$D_{zz} = \frac{2}{3}D$$

$$D = \frac{3D_{zz}}{2}$$

$$E = \frac{D_{xx} - D_{yy}}{2} \quad (7)$$

Note that the absolute signs of the D and E parameters in Table 1 are unknown. It is only known that D and E have the same sign in each case. Changing the signs of both D and E at the same time will not result in a different EPR simulation of the high–temperature spectra. When doing so, the simulated intensity pattern, but not the resonance positions will change if the Zeeman energy is comparable to kT, which is the basis of the D sign determination in HFEPR.[25,26]. Unfortunately, at temperatures low enough for this effect to become important in the powder HFEPR spectra, our antiferromagnetic complexes show no EPR signals due to the depopulation of the magnetic states. We cannot therefore determine the sign of D in any of the S states. The relative sign of the S = 1 parameters versus the S = 2 parameters is important; thus, we need to consider sets in which the S = 1 parameters $D_{S=1}$ and $E_{S=1}$ have the sign either the same or opposite to the S = 2 parameters $D_{S=2}$ and $E_{S=2}$ The set $D_{S=1} = -4.776$ cm^{-1}, $E_{S=1} = -0.359$ cm^{-1}, $D_{S=2} = 0.259$ cm^{-1}, $E_{S=2} = 0.036$ cm^{-1} appeared to produce more reasonable results (shown below) than a set with all positive D and E values.

Converting the D and E values above into the respective diagonal ZFS tensors elements using formulas (7), we get a set of the diagonal D_{xx}, D_{yy}, D_{zz} tensor elements for $\{\boldsymbol{D}_{S=1}\}$ and $\{\boldsymbol{D}_{S=2}\}$:

	D_{xx} (cm^{-1})	D_{yy} (cm^{-1})	D_{zz} (cm^{-1})
$\{\boldsymbol{D}_{S=1}\}$	1.233	1.951	−3.184
$\{\boldsymbol{D}_{S=2}\}$	−0.0533	−0.1223	0.1727

But since we know that the $\{\boldsymbol{D}_{S=2}\}$ tensor has its Z axis parallel to the Y axis of the $\{\boldsymbol{D}_{S=1}\}$ tensor, we need to swap its yy and zz elements:

	D_{xx} (cm^{-1})	D_{yy} (cm^{-1})	D_{zz} (cm^{-1})
$\{\boldsymbol{D}_{S=1}\}$	1.233	1.951	−3.184
$\{\boldsymbol{D}_{S=2}\}$	−0.0533	0.1727	−0.1223

Using relations (6) one can now find the tensors $\{\mathbf{D}_{12}\}$, $\{\mathbf{D}_{Fe}\} = \{\mathbf{D}_{Fe1}\} = \{\mathbf{D}_{Fe2}\}$ and the $\{\mathbf{D}_{S=3}\}$ tensor resulting from them:

	D_{xx} (cm^{-1})	D_{yy} (cm^{-1})	D_{zz} (cm^{-1})
$\{\boldsymbol{D}_{Fe}\}$	−0.514	−0.465	0.975
$\{\boldsymbol{D}_{12}\}$	−0.556	−0.276	0.826
$\{\boldsymbol{D}_{S=3}\}$	−0.268	−0.124	0.388

The scalar parameters D and E resulting from these tensors are:

$D_{Fe} = -1.462$ cm^{-1}, $E_{Fe} = -0.025$ cm^{-1}, $D_{12} = -1.242$ cm^{-1}, $E_{12} = -0.140$ cm^{-1}, $D_{S=3} = 0.584$ cm^{-1}, $E_{S=3} = -0.072$ cm^{-1}.

A spectrum of the phen complex simulated by using the microscopic spin Hamiltonian (5) with $J = 190$ cm^{-1} and D_{Fe}, E_{Fe}, D_{12}, E_{12} listed above is shown in Figure 9.

The S = 3 parameter set so obtained is somewhat similar to the experimental set in Table 1. In ref [11], a set $D_{Fe} = -1.77$ cm^{-1}, $E_{Fe} = -0.026$ cm^{-1}, $D_{12} = -1.465$ cm^{-1}, $E_{12} = -0.026$ cm^{-1} was found from the analysis of the S = 2 and S = 3 spectra. Considering the complexity of the problem and the simplifications applied both here and in ref [11], the agreement seems reasonable.

The surprising finding is the large value of the anisotropic interaction parameters, D_{12} and E_{12}. The magnetic dipole–dipole interaction and the anisotropy of the exchange interactions contribute to these parameters. The dipole–dipole contribution to D_{12} equals

$$D_{dip} = -3\frac{g^2\mu_B^2}{R_{12}^3} \quad (8)$$

With the Fe–Fe distance R_{12} of 3.49 A, D_{dip} evaluates to −0.12 cm^{-1} and clearly it is overwhelmed by the anisotropic exchange contribution, as the total D_{12} is −1.24 cm^{-1}. Depending on the orientation of the $\{\boldsymbol{D}_{dip}\}$ tensor versus the $\{\boldsymbol{D}_{Fe}\}$ tensor, the dipolar interaction may contribute to $D_{S=3}$ between (47/

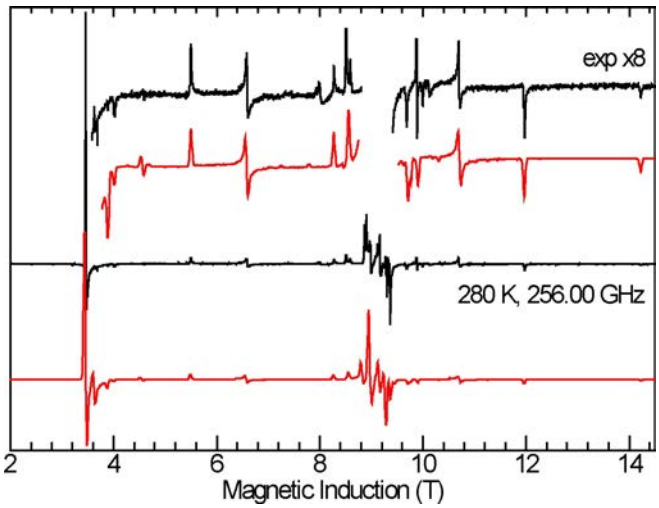

Figure 9. HFEPR spectrum of $[Fe(phen)_2(H_2O)]_2O(NO_3)_4 \cdot 5H_2O$. Black: experimental; red: simulated by using the microscopic spin Hamiltonian (5) with $J = 190$ cm^{-1}, $D_{Fe} = -1.462$ cm^{-1}, $E_{Fe} = -0.025$ cm^{-1}, $D_{12} = -1.242$ cm^{-1}, $E_{12} = -0.140$ cm^{-1}. When using the reported value $J = 220$ cm^{-1}, the S = 2 resonance intensity was suppressed too strongly.

90)·(−0.12 cm^{-1}) = −0.064 cm^{-1} and (47/90)·0.06 cm^{-1} = 0.032 cm^{-1}. The former number applies to the case of the two tensors' Z axes being parallel, and the latter number is for the case of a perpendicular orientation. The dipolar interaction contributes thus at most 10% of the observed $D_{S=3}$ and substantial anisotropic exchange must be present. Note also that the coefficient before the $\{\boldsymbol{D}_{Fe}\}$ tensor in formula 6a for $\{\boldsymbol{D}_{S=3}\}$ is very small (2/45). The ZFS in S = 3 is thus indeed mainly determined by $\{\boldsymbol{D}_{12}\}$ as its coefficient is 11.75 times larger. Hence, a large value of $D_{S=3}$ implies a significant anisotropy of the exchange interactions. The theory of the anisotropic exchange has been developed in relatively recent past for the dimeric Cu(II) complexes.[27,] The exchange–related contribution to D is caused by the spin–orbit coupling of the ground state of the dimer to its electronically excited states. This should not produce a large contribution for Fe^{3+} whose ^6S term does not split in the ligand field and is not subject to the spin–orbit interaction. Nevertheless, large $D_{exchange}$ contributions have been observed here and in ref [11], and previously ter Heerdt *et al.*[28] have performed a single–crystal study on a doubly bridged Fe^{3+} dimer to find $D_{exchange}$ of −0.14 cm^{-1}, which is an order of magnitude smaller than that found in this work, but their complex exhibited the isotropic exchange of only 15 cm^{-1}, compared to ~200 cm^{-1} in the present work. Although no exchange contribution to $\{\boldsymbol{D}_{12}\}$ is given in ref [16], the pattern of the D_S values in the S = 1, 2 and 3 states–largest $D_{S=1}$, small $D_{S=2}$ and $D_{S=3}$ larger than the latter one also indicates a substantial exchange contribution to $\{\boldsymbol{D}_{12}\}$.

The model relating the "giant spin" and the "microscopic" Hamiltonian is imperfect in practice. When the parameters of only two spin states of a binuclear system are known, local ZFS and interaction–related ZFS contributions can be determined,[11] as there are 2 equations with 2 unknowns. This may be misleading, however: when parameters of more spin states are known, like in this paper or in dimeric Cr(III)[29,30] or Mn(IV),[31] it is found that it may be impossible to fit them all with one set of the $\{\boldsymbol{D}_{metal}\}$ and $\{\boldsymbol{D}_{12}\}$ tensors. A very serious problem is the non–parallel axes of the various tensors involved, like $\{\boldsymbol{Fe}_1\}$ and $\{\boldsymbol{Fe}_2\}$ tensors in systems where the two metal ions are not symmetry related, and their relation to the axes of the anisotropic exchange tensor. A perfect agreement may thus not be achieved. Still, the unexpectedly large exchange contribution appears to be real, since as shown above, a large zero–field splitting in the S = 3 state implies a significant exchange contribution even without performing the operations on tensors described here.

Conclusions

HFEPR study performed on three binuclear μ–oxo bridged iron(III) complexes allowed accurate determination of the spin Hamiltonian parameters for the excited S = 1, S = 2 and S = 3 states. Also, the microscopic spin Hamiltonian was employed with partial success to simulate the HFEPR spectra of $[Fe(phen)_2(H_2O)]_2O(NO_3)_4 \cdot 5H_2O$. Interestingly, most of the EPR spectra in this work were obtained at room temperature with excellent quality. The general expectation of EPR spectroscopists that low temperature would help to produce better spectra is not applicable here. The parameters for S = 1 could not be determined in the past using standard X–Band and Q–Band EPR techniques owing to extremely large zero–field splitting. An unexpectedly large contribution to ZFS due to anisotropic exchange interactions was found for all complexes examined in this work. The FeOFe bridge motif studied in this work is encountered in some important biological systems, sometimes accompanied by a second bridge (carboxylate).[1,2,5–8,13] A HFEPR investigation of such systems may be worthy of trying.

Acknowledgements

This work was performed at the National High Magnetic Field Laboratory which is supported by the National Science Foundation Cooperative Agreement No. DMR–2128556 and DMR-1644779, and the State of Florida. The author thanks Dr. Tomas Orlando of the NHMFL for recording the room temperature X–Band EPR spectra of $Na_4[Fe(edta)]_2O \cdot 3H_2O$ and $[Fe(phen)_2(H_2O)]_2O(NO_3)_4 \cdot 5H_2O$.

Conflict of Interests

The authors declare no conflict of interest.

Data Availability Statement

The data that support the findings of this study are available in the supplementary material of this article.

[1] K. S. Murray, *Coord. Chem. Rev.* **1974**, *12*, 1–35.
[2] D. M. Kurtz Jr., *Chem. Rev.* **1990**, *90*, 585–606.
[3] E. Nordlander, A. Thapper, J. King, C. Lorber, H. Carlsson, F. Prestopino, N. Focci, *Coord. Chem. Rev.* **1995**, *1998*(172), 3–97.
[4] T. Glaser, *Coord. Chem. Rev.* **2019**, *380*, 353–377.
[5] T. Guchhait, S. Sasmal, F. Shah, T. Khan, S. P. Rath, *Coord. Chem. Rev.* **2017**, *337*, 112–144.
[6] S. Walleck, T. Glaser, *Isr. J. Chem.* **2020**, *60*, 1019–1031.
[7] M. L. Caldas Nogueira, A. J. Pastore, V. L. Davidson, *Arch. Bioch. Bioph.* **2021**, *705*, 108917.
[8] T. C. Brunold, E. I. Solomon, *J. Am. Chem. Soc.* **1999**, *121*, 8277–8287.
[9] G. N. La Mar, G. R. Eaton, R. H. Holm, F. A. Walker, *J. Am. Chem. Soc.* **1973**, *95*, 63–75.
[10] M. Y. Okamura, B. M. Hoffman, *J. Chem. Phys.* **1969**, *51*, 3128–3129.
[11] A. Ozarowski, B. R. McGarvey, J. E. Drake, *Inorg. Chem.* **1995**, *34*, 5558–5566.
[12] H. Schugar, G. R. Rossman, C. G. Barraclough, H. B. Gray, *J. Am. Chem. Soc.* **1972**, *94*, 2683–2690.
[13] J. E. Plowman, T. M. Loehr, C. K. Schauer, O. P. Anderson, *Inorg. Chem.* **1984**, *23*, 3553–3559.
[14] a) P. Coggon, A. T. McPhail, P. M. Gross, F. E. Mabbs, V. N. McLachlan, *J. Chem. Soc. (A)* **1971**, 1014–1019; b) R. G. Wollmann, D. N. Hendrickson, *Inorg. Chem.* **1977**, *16*, 723–733.
[15] a) A. Bencini, D. Gatteschi, *In EPR of Exchange CoupledSystems*, Springer Verlag, Berlin/Heidelberg **1990**; b) A. Abragam, B. Bleaney, *In Electron Paramagnetic Resonance of Transition Ions*, Clarendon Press, Oxford **1970**.
[16] S. J. W. Holgate, G. Bondarenko, D. Collison, F. E. Mabbs, *Inorg. Chem.* **1999**, *38*, 2380–2385.

[17] K. W. H. Stevens, *Proc. Phys. Soc.* **1952**, *A65*, 209–215.
[18] J. J. TelserKrzystek, J. Krzystek, A. Ozarowski, *Resonance* **2012**, *23*, 209–263.
[19] D. M. de Souza Esquivel, A. Siuiti Ito, S. Isotani, *J. Phys. Soc. Jpn.* **1976**, *40*, 947–954.
[20] a) Ming Li, W. R. Scheidt, *J. Porphyrins Phthalocyanines* **2020**, *24*, 1105–1112; b) H. M. Refaat, A. A. M. Alotaibi, N. Dege, A. El–Faham, S. M. Soliman, *Inorg. Chim. Acta* **2022**, *504*, 121196; c) N. Panza, A. di Biase, A. Caselli, *Inorg. Chim. Acta* **2022**, *541*, 121091; d) L. P. Cailler, M. Clémancey, J. Barilone, P. Pascale Maldivi, J.-M. Latour, A. B. Sorokin, *Inorg. Chem.* **2020**, *59*, 1104–1116; e) J. Bernhardette, H. Strautmann, S. Dammers, T. Limpke, J. Parthier, T. P. Zimmermann, S. Walleck, G. Heinze–Brückner, A. Stammler, H. Bögge, T. Glaser, *Dalton Trans.* **2016**, *45*, 3340.
[21] J. E. Davies, B. M. Gatehouse, *Acta Cryst.* **1973**, *B29*, 1934–1941.
[22] A. Hassan, L. Pardi, J. Krzystek, A. Sienkiewicz, P. Goy, M. Rohrer, L.–C. Brunel, *J. Magn. Reson.* **2000**, *142*, 300–312.
[23] A. Ozarowski, EPR simulation program for $S > 1/2$, https://osf.io/z72tg/.
[24] A. V. Khedekar, J. Lewis, F. E. Mabbs, H. J. Weigold, *J. Chem. Soc. A* **1967**, 1561–1564.
[25] A. Ozarowski, C. J. Calzado, R. P. Sharma, S. Kumar, J. Jezierska, C. Angeli, F. Spizzo, V. Ferretti, *Inorg. Chem.* **2015**, *54*, 11916–11934.
[26] A. Ozarowski, *Inorg. Chem.* **2008**, *47*, 9760–9762.
[27] R. Maurice, K. Sivalingam, D. Ganyushin, N. Guihéry, C. De Graaf, F. Neese, *Inorg. Chem.* **2011**, *50*, 6229–6236.
[28] P. Ter Heerdt, M. Stefan, E. Goovaerts, A. Caneschi, A. Cornia, *J. Magn. Reson.* **2006**, *179*, 29–37.
[29] T. J. Morsing, H. Weihe, J. Bendix, *Inorg. Chem.* **2016**, *55*, 1453–1460.
[30] V. V. Semenaka, O. V. Nesterova, V. N. Kokozay, V. V. Dyakonenko, R. I. Zubatyuk, O. V. Shishkin, R. Boča, J. Jezierska, A. Ozarowski, *Inorg. Chem.* **2010**, *49*, 5460–5471.
[31] D. Premuzic, M. Holynska, A. Ozarowski, C. Pietzonka, A. Roseborough, S. A. Stoian, *Inorg. Chem.* **2020**, *59*, 10768–10784.

Manuscript received: September 1, 2024
Revised manuscript received: October 19, 2024
Accepted manuscript online: October 23, 2024
Version of record online: ■■, ■■

RESEARCH ARTICLE

High-Field EPR allows to determine the zero-field splitting (ZFS) parameters *D* and *E* in three antiferromagnetic binuclear μ-oxo bridged iron(III) complexes. The ZFS in the first excited spin state with spin S = 1 is very large, far beyond the reach of the standard X or Q-Band EPR.

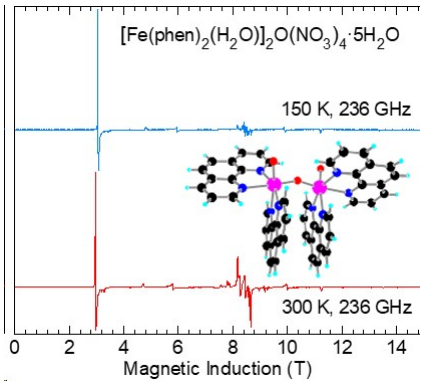

*A. Ozarowski**